SLOVAK UNIVERSITY OF TECHNOLOGY
IN BRATISLAVA

FACULTY OF CHEMICAL AND FOOD TECHNOLOGY

Reg. No.: FCHPT-16584-105389

Advanced Control of a Laboratory Distillation Column

MASTER THESIS

2025 **Bc. Marko Micherda**

SLOVAK UNIVERSITY OF TECHNOLOGY IN BRATISLAVA

FACULTY OF CHEMICAL AND FOOD TECHNOLOGY

Reg. No.: FCHPT-16584-105389

Advanced Control of a Laboratory Distillation Column

MASTER THESIS

Study programme:	Process Control
Study field:	Cybernetics
Training workspace:	Department of Information Engineering and Process Control
Thesis supervisor:	doc. Radoslav Paulen, PhD.

2025

Bc. Marko Micherda

Slovak University of Technology in Bratislava
Department of Information Engineering and Process Control

Faculty of Chemical and Food Technology
Academic year: 2024/2025
Reg. No.: FCHPT-16584-105389

STU FCHPT

MASTER THESIS TOPIC

Student:	**Bc. Marko Micherda**
Student's ID:	105389
Study programme:	Automation and Information Engineering in Chemistry and Food Industry
Study field:	Cybernetics
Thesis supervisor:	doc. Ing. Radoslav Paulen, PhD.
Head of department:	
Workplace:	Oddelenie informatizácie a riadenia procesov FCHPT STU

Topic: **Advanced Control of a Laboratory Distillation Column**

Language of thesis: English

Specification of Assignment:

Distillation columns are among the most important units in the process industry. The quality of their control can have a significant impact on overall profitability. The complexity of industrial distillation columns often make it difficult to effectively analyze various advanced control strategies. The objective of this work is to design an advanced controller for the UOP3CC laboratory distillation column and compare its control performance with a basic control structure consisting of individual PI controllers.

Selected bibliography:

1. SKOGESTAD, Sigurd. *Chemical and Energy Process Engineering.* Boca Raton : CRC Press, 2008. 436 p. ISBN 978-1-4200-8755-0.
2. SKOGESTAD, Sigurd; POSTLETHWAITE, Ian. *Multivariable Feedback Control: Analysis and Design.* Chichester : John Wiley & Sons, 2005. 574 p. ISBN 0-470-01168-8.

Deadline for submission of Master thesis:	16. 05. 2025
Approval of assignment of Master thesis:	06. 03. 2025
Assignment of Master thesis approved by:	prof. Ing. Miroslav Fikar, DrSc. – Study programme supervisor

Honour Declaration

I declare that the submitted diploma thesis was completed on my own, in cooperation with my supervisor, with the help of professional literature and other information sources, which are cited in my thesis in the reference section. As the author of my diploma thesis, I declare that I didn't break any third party copyrights.

.....

Signature

Acknowledgment

I would like to express my deepest gratitude to my supervisor doc. Ing. Radoslav Paulen, PhD. for his invaluable guidance and support throughout this semester. His expertise, patience, and encouragement have been instrumental in the successful completion this work.

Abstract

This thesis focuses on the analysis, control, and modeling of a laboratory distillation column used for the separation of a methanol–water mixture. The main objective was to design and implement a PI temperature controller to regulate the temperatures at the top and bottom of the column, ensuring stable operation. The PI controllers were tuned using the Skogestad method, which involves deriving transfer functions and calculating suitable control parameters based on the system dynamics. A state-space model was subsequently derived, which served as the basis for designing advanced LQR control, more suitable for multi-input multi-output (MIMO) systems.

In addition, the thesis explores the use of simulation software, specifically AVEVA and gPROMS, for modeling the distillation process. The models were developed to replicate the behavior of the real column under steady-state conditions. The results were validated by comparing simulated and experimental temperature profiles, and simulation parameters were also used to estimate variables that cannot be directly measured in the laboratory column. The thesis highlights the importance of control system design and process modeling in the optimization of distillation operations and provides valuable insights into the integration of experimental data with advanced simulation tools.

Keywords: distillation column, PI controller, LQR control, AVEVA, gPROMS Process builder

Abstrakt

Táto diplomová práca sa zameriava na analýzu, riadenie a modelovanie laboratórnej destilačnej kolóny na separáciu zmesi metanolu a vody. Hlavným cieľom bolo navrhnúť a implementovať PI regulátor teploty na riadenie teplôt na vrchu a dne kolóny s cieľom zabezpečiť stabilnú prevádzku. PI regulátory boli ladené pomocou Skogestadovej metódy, ktorá zahŕňa odvodenie prenosových funkcií a výpočet vhodných regulačných parametrov na základe dynamiky systému. Následne bol odvodený stavový model, na základe ktorého bolo navrhnuté pokročilé LQR riadenie, ktoré je vhodnejšie pre systémy s viacerými vstupmi a výstupmi.

Okrem toho sa práca zaoberá využitím simulačných softvérov, konkrétne AVEVA a gPROMS, na modelovanie destilačného procesu. Modely boli vytvorené s cieľom replikovať správanie skutočnej kolóny za ustálených podmienok. Výsledky boli overené porovnaním simulovaných a experimentálnych teplotných profilov a parametre simulácií poslúžili aj na odhad veličín, ktoré nie je možné priamo zmerať na laboratórnej kolóne. Práca zdôrazňuje význam návrhu riadiacich systémov a modelovania procesov pri optimalizácii destilačných operácií a poskytuje cenné poznatky o integrácii experimentálnych údajov s pokročilými simulačnými nástrojmi.

Kľúčové slová: destilačná kolóna, PI regulátor, LQR riadenie, , AVEVA, gPROMS Process builder

Contents

Chapter 1

Introduction

1.1 The Importance of Distillation Columns

Distillation columns have long been among the most important equipment in the chemical and food industries. Information about this process dates back to approximately the 1st century AD, but distillation was not used on a larger scale until the 11th century to increase the ethanol content in alcoholic beverages. These devices are essential tools for separating mixtures into individual components based on differences in their volatility. Thanks to this process, we can ensure effective isolation of substances, which is crucial for the production of high-quality and pure products [3], [8], [16].

Today, oil refineries are indispensable without distillation columns. They play a crucial role in the separation of crude oil into various fractions, such as gasoline, lubricating oils, diesel fuel, and kerosene. The range of products in industrial facilities is diverse, from a few kilograms per hour in laboratory columns with a height of about one meter to hundreds of kilotons per hour, where columns reach a height of several tens of meters [10].

Another important application of distillation columns is in the pharmaceutical industry. Here, they are used to remove reaction by-products and obtain pure substances. Similarly, in the food industry, distillation is used to produce aromas, essential oils, alcoholic beverages by the separation of ethanol from water and other impurities and other ingredients that are important for the quality of food products[4].The distillation process is a major component of investment in chemical processes and refineries worldwide, and the operating costs of distillation columns are often a major part of a company's total costs. [15].

Because this is a very complex device, proper control of distillation units is crucial to achieve maximum product yield with minimal energy consumption. The control of such systems presents significant problems and uncertainties due to their multidimensional

nature, nonlinear behavior, and the presence of non-idealities, such as deviations from equilibrium, heat loss to the environment, especially if the column is outdoors during changing seasons or imperfect mixing. Advanced control strategies are needed to solve these complex problems. Therefore, in my thesis, I would like to dedicate myself to the design of an advanced control that will ensure the efficient and safe operation of a laboratory distillation column, which is located at the Institute of Informatics and Automation of the Slovak University of Technology in Bratislava [10], [3].

1.2 Goals of the Thesis

The primary goal of this thesis is to develop an advanced control strategy for a laboratory distillation column. To achieve this, the work focuses on:

1. Designing and validating a reliable process model for the distillation column that integrates both steady-state and dynamic behavior.
2. Exploring optimization techniques to improve the column's operational efficiency and ensure robust performance under varying conditions.
3. Implementing and testing advanced control strategies, to achieve enhanced process stability and product quality.
4. Compare simulation results with experimental data to ensure that the proposed control strategies are applicable in real-world laboratory settings.

This thesis aims to contribute to the field of process control by demonstrating the integration of modeling, temperature control, and experimentation in the development of innovative control solutions.

Chapter 2

Theoretical Background

2.1 Basics of Distillation and Operation of a Distillation Column

Distillation is a thermal separation process. It exploits the differences in the volatility of the components. The more volatile component has a lower boiling point and the less volatile component has a higher boiling point. When we bring our mixture to the boiling point, the vapor that is formed begins to be saturated more with the more volatile component and rises upward, where it is condensed to obtain a liquid distillate. Conversely, the less volatile component remains more in the liquid phase, and its concentration increases downwards with the flow of liquid in the column. This vapor-liquid system is governed by the principles of phase equilibrium, specifically vapor-liquid equilibrium (VLE) [4], [16].

In the case of a binary mixture, the relationship between the vapor and liquid compositions at equilibrium can be described by Raoult's law:

$$y_i P = x_i P_i^* \quad \text{for } i = 1, 2, \ldots, n, \tag{2.1}$$

where y_i and x_i are the mole fractions of component i in the vapor and liquid phases, respectively. Here, P represents the total system pressure, and P_i^* is the vapor pressure of the pure component i at the system temperature.

The total vapor pressure above a liquid mixture is given by the sum of the partial pressures of the individual components [7]. The vapor phase is created by raising the temperature of the liquid mixture until some of the liquid evaporates, forming a vapor-liquid mixture. The dynamic interaction between the phases drives the separation process [22].

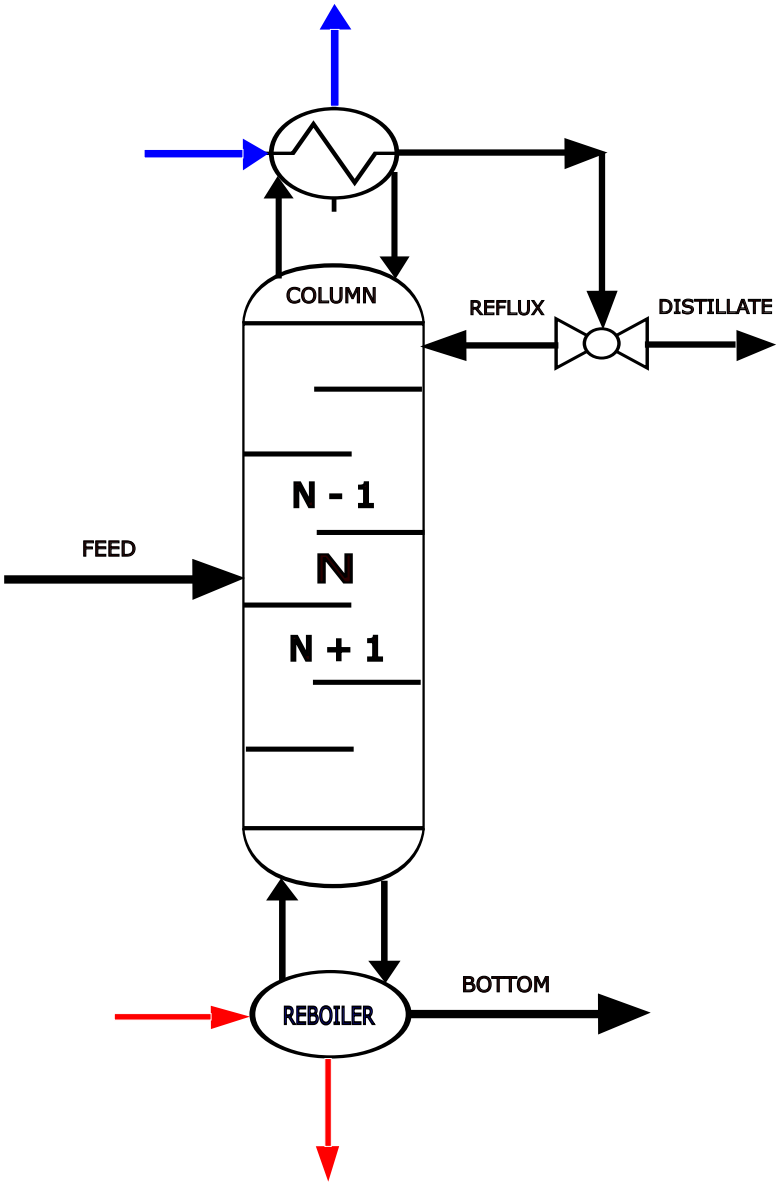

Figure 2.1: Scheme of a distillation column

2.2 Classification of Distillation Column Parameters

Understanding the behavior of a distillation column starts with properly categorizing the parameters that influence it. These parameters can be divided according to their characteristics and the context in which they are applied during design or operation. They generally fall into three main groups: variables that are continuously adjusted during operation, parameters that are set during the design phase, and output indicators that reflect the performance of the system. Each of these plays a important role in shaping the efficiency and dynamics of the column [15].

1. **Continuous Degrees of Freedom (Operational Parameters):** These parameters can be adjusted during the operation of the column to influence its performance:
    - **Reflux Ratio:** This parameter defines the proportion between the liquid that is recirculated back into the column and the distillate withdrawn as product. Increasing the reflux ratio typically improves the separation quality, resulting in higher energy demands [23].
    - **Heat Supplied to the Reboiler:** The thermal energy introduced into the reboiler governs the amount of vapor generated, which in turn has a significant impact on the separation performance.
    - **Heat Removed in the Condenser:** This controls the condensation process at the top of the column, enabling efficient reflux formation, consistent collection of distillate and stable column pressure [13].
2. **Design Parameters:** These parameters are determined during the design stage of the column and are typically not adjusted during operation:
    - **Number of Theoretical Stages:** The number of equilibrium stages required for a given separation of mixture, often estimated using graphical methods such like the McCabe-Thiele method.
    - **Column Geometry and Internal Design:** Includes tray specifications, column height, and diameter, which directly influence the column's capacity and efficiency.
3. **Performance Metrics (Output Parameters):** These parameters reflect the overall effectiveness of the column under given operating conditions:
    - **Efficiency:** Includes overall column efficiency and individual stage efficiencies. It is influenced by factors such as tray design, packing material, and operational conditions [2].

- **Product Purity:** The molar or mass fraction of key components in the distillate and bottom products serves as key indicators of column separation efficiency [13].

2.3 Control Strategies

The control of the distillation columns plays a key role in the operation of these devices. To achieve the desired product quality and safety, we need to design a controller that ensures that one or more outputs of the system behave in the desired way. To ensure this, our controller must correctly handle the manipulated variable or compensate for disturbances [21].

2.3.1 Discrete PID Controllers

Discrete proportional-integral-derivative (PID) controllers are commonly applied in the control of distillation columns because they offer straightforward design and reliable performance. Nowadays, more than 90% control loops are still controlled by these regulators. In most cases, only a PI regulator is used, where the derivative part is equal to zero [9]. They play a crucial role in the adjustment of manipulated variables in distillation, such as the heat input of the reboiler, the reflux flow rate, or the cooling duty of the condenser, to minimize the error between the set point (the desired value) and the measured variable [11].

The control law governing discrete PID controller is expressed as:

$$u[k] = K_p \cdot e[k] + K_i \cdot \sum_{i=0}^{k} e[i] \cdot T_s + K_d \cdot \frac{e[k] - e[k-1]}{T_s} \tag{2.2}$$

where $u[k]$ is the control output at the discrete time step k, $e[k]$ represents the control error, defined as the difference between the reference value $r[k]$ and the measured process output $y[k]$. K_p, K_i, and K_d are the proportional, integral, and derivative gains, T_s describes the sampling period, which is the time interval between two discrete steps [15].

2.3.1.1 Pairing Analysis for PID Control

A PID controller is a type of controller that can provide control of systems that are SISO, or single-input single-output. In a device like a distillation column which is a

MIMO system, or multiple-input multiple-output, we need to ensure proper pairing of the variables. In a distillation column, there are many different options for controlling the temperature in the column, but the most widely used in industry is *LV configuration* [5]:

- **L (Reflux Flow):** The liquid flow that returns to the column regulates the quality of separation.
- **V (Vapor Flow):** The boil-up rate, controlled by the reboiler heat input, adjusts the column energy balance [4].

The theory of automatic control recommends pairing controlled and manipulated variables based on the Relative Gain Array (RGA) to minimize interactions. Typically, the temperature on the top is controlled by reflux flow (L), while the temperature of the bottom product is controlled using the vapor flow (V) or duty of the reboiler when we use electric heating [1].

The relative gain array (RGA) matrix, decribed as Λ, is defined as:

$$\Lambda = G \circ (G^{-1})^T$$

,where G is the steady-state gain matrix and $\circ$ denotes the Hadamard (element-wise) product [6].

2.3.2 Advanced Control

Advanced process control (APC) techniques are better suited than traditional PID controllers by offering more effective solutions for managing the challenges associated with complex, nonlinear and multivariate distillation systems. Unlike basic PID approaches, which can struggle with interactions between variables and dynamic changes, APC strategies are specifically designed to handle these difficulties with greater precision. By incorporating predictive models and coordinated control actions, APC methods significantly improve process stability, reduce variability, and optimize overall plant performance [17].

2.3.2.1 Discrete Linear Quadratic Controller

The discrete linear quadratic regulator (LQR) is an optimal control technique that determines feedback signals for linear dynamic systems by minimizing a predefined

quadratic cost function and balancing the performance of the system with the control effort. The mathematical expression of LQR can be interpreted using the cost function [20]:

$$J = \sum_{k=0}^{\infty} \left(x[k]^\top Q\, x[k] + u[k]^\top R\, u[k] \right) \tag{2.3}$$

where x is the state vector in time step k, u is the control input at time step k, $Q \succeq 0$ is the state weighting matrix, and $R \succ 0$ is the input weighting matrix.

The general state-space representation of a linear discrete system is given by:

$$\mathrm{x}[k+1] = \mathrm{A}\,\mathrm{x}[k] + \mathrm{B}\,\mathrm{u}[k] \tag{2.4}$$

$$\mathrm{y}[k] = \mathrm{C}\,\mathrm{x}[k] + \mathrm{D}\,\mathrm{u}[k] \tag{2.5}$$

where y is the output vector at time step k, and A, B, C, D are the system matrices.

For proper functioning of the control system, it is essential to ensure the correct values of the input vector u, which is defined as:

$$\mathrm{u}[k] = -K \cdot x[k] \tag{2.6}$$

The matrix K is the state feedback gain matrix, which is designed to place the closed-loop poles of the system at desired locations, ensuring the stability and desired dynamic performance. It is calculated as [20]:

$$K = \left(R + B^\top P B \right)^{-1} B^\top P A \tag{2.7}$$

where P is the solution to the Discrete Algebraic Riccati Equation (DARE):

$$P = A^\top P A - A^\top P B \left(R + B^\top P B \right)^{-1} B^\top P A + Q \tag{2.8}$$

Let us define $x_i[k]$ as the integral (in discrete form, a sum) of the output error:

$$x_i[k+1] = x_i[k] + Ts \cdot (r[k] - y[k]) = x_i[k] + Ts \cdot r[k] - Ts \cdot Cx[k]$$

The extended state vector is constructed in the following form:

$$x_a[k] = \begin{bmatrix} x[k] \\ x_i[k] \end{bmatrix}$$

This leads to the following augmented state-space formulation:

$$x_a[k+1] = \begin{bmatrix} A & 0 \\ -Ts * C & I \end{bmatrix} x_a[k] + \begin{bmatrix} B \\ 0 \end{bmatrix} u[k] + \begin{bmatrix} 0 \\ I \end{bmatrix} r[k]$$

Control law

The LQR regulator for the extended system can be written as:

$$u[k] = -\begin{bmatrix} K_x & K_i \end{bmatrix} \begin{bmatrix} x[k] \\ x_i[k] \end{bmatrix}$$

where K_x is the gain for the original states, and K_i is the gain for the integral state [18].

Discrete state observer

When not all internal states of a system are directly measurable, it is necessary to estimate them using a state observer. To estimate the unmeasured states, an observer is constructed with the following structure:

$$\hat{x}[k+1] = A_d\hat{x}[k] + B_d u[k] + L(y[k] - \hat{y}[k]), \tag{2.9}$$

$$\hat{y}[k] = C_d\hat{x}[k] + D_d u[k], \tag{2.10}$$

where, $\hat{x}[k]$ represents the estimated states, $\hat{y}[k]$ is the estimated output, and L is the observer gain matrix. The expression $y[k] - \hat{y}[k]$ represents the estimation error, which the observer uses to correct its prediction [18].

The gain of the observer L has to be chosen such that the eigenvalues of the matrix $A_d - LC_d$ are inside the unit circle in the complex plane to ensure the convergence of the estimates:

$$\text{eig}(A_d - LC_d) \in D, \tag{2.11}$$

where D describes the unit disk.

The pole placement method or optimal estimation, such as the Kalman filter in discrete time, can be used to determine the appropriate gain matrix L. This estimated state can then be used in LQR controllers, where full state feedback is necessary [18].

2.3.2.2 Model Predictive Control (MPC):

MPC is one of the most widely used advanced control strategies in distillation. Using a dynamic process model, it predicts future system behavior and optimizes control actions within a given time horizon. Taking into account multivariate interactions and system constraints, MPC effectively manages disturbances and achieves tight control of product compositions and energy usage. The main difference between the MPC controller and the LQR controller lies in the constraints and the prediction of the future. The MPC can work directly with constraints for both inputs and outputs and can also predict future actions. On the other hand, the MPC needs more computational power since it performs optimization within itself, and the advantage of the LQR is also that it can operate in offline mode, so we only need to calculate its parameters in the form of matrices once. The control objective can be represented as [3], [7]:

$$\min J = \sum_{k=1}^{N} \left(\|y_k - y_{\text{set}}\|^2 + \lambda \|\Delta u_k\|^2 \right), \tag{2.12}$$

where J is the cost function, y_k is the predicted output, y_{set} is the setpoint, Δu_k is the control input change, and λ is a weighting factor [7].

2.4 Theory of Distillation Column Modeling

To ensure effective control and optimization of a distillation column, a clear understanding of its physical and chemical processes is essential. This understanding is achieved

through modeling, which serves as the foundation for both design and operational strategies. An accurate process model allows us to design a controller, thanks to which we can achieve our outputs at the desired values, which can save operating costs but also improve the safety of the equipment. The equations used in this section are derived from the gPROMS Process Builder manual [13], reflecting the mathematical framework used by the software to simulate the dynamics of the distillation column. These equations provide the necessary tools to predict the performance of the column.

2.4.1 Mass Balance and Energy Balance

The mass and energy balance for component i in the liquid phase is expressed as:

$$\begin{aligned}\hat{V}_j \frac{d\bar{m}_{i,j}}{dt} &= L_{j-1}x_{i,j-1} + V_{j+1}y_{i,j+1} + F_j^L x_{i,j}^L + F_j^V y_{i,j}^V \\ &\quad - (1 + S_{\text{frac},j}^L)L_j x_{i,j} - (1 + S_{\text{frac},j}^V)V_j y_{i,j}, \quad \forall i \in C, \quad j = 1, \ldots, N \end{aligned} \tag{2.13}$$

$$\frac{x_{i,j}}{M_{w_i}}\phi_{i,j}^L = \frac{y_{i,j}}{M_{w_i}}\phi_{i,j}^V, \quad \forall i \in C, \quad j = 1, \ldots, N \tag{2.14}$$

$$\sum_{i \in C} x_{i,j} = 1, \quad \forall j = 1, \ldots, N \tag{2.15}$$

$$\sum_{i \in C} y_{i,j} = 1, \quad \forall j = 1, \ldots, N \tag{2.16}$$

$$\begin{aligned}\hat{V}_j \frac{d\hat{u}_j}{dt} &= L_{j-1}h_{j-1}^L + V_{j+1}h_{j+1}^V + h_L^F F_j^L + h_V^F F_j^V \\ &\quad - (1 + S_{\text{frac},j}^L)L_j h_j^L - (1 + S_{\text{frac},j}^V)V_j h_j^V, \quad \forall j = 1, \ldots, N \end{aligned} \tag{2.17}$$

The material and energy holdups are defined below (note that subscript j has been omitted for readability):

$$M_i = M^L x_i + M^V y_i, \qquad \forall i \in C \tag{2.18}$$

$$\frac{M^L}{\rho_L} + \frac{M^V}{\rho_V} = \hat{V} \tag{2.19}$$

$$\hat{u} = \bar{\boldsymbol{m}}^T H - 10^2 P \tag{2.20}$$

$$\bar{\boldsymbol{m}}^T H \hat{V} = M^L h^L + M^V h^V \tag{2.21}$$

$$\sum_{\forall i \in C} M_i = M^T \tag{2.22}$$

Murphree efficiency

Murphree efficiency can be used to account for non-ideal equilibrium conditions on each tray. It is defined as:

$$E_{M,i,j}^{V} = \left(\frac{y_{\text{molar},i,j} - y_{\text{molar},i,j-1}}{y_{\text{molar},i,j}^{*} - y_{\text{molar},i,j-1}} \right), \quad \forall i \in C, \quad j = 1, \ldots, N \tag{2.23}$$

2.4.2 Phase Equilibrium: NRTL Model

The phase equilibrium in a distillation column is essential for determining the concentration of components. The Non-Random Two-Liquid (NRTL) model is used in gPROMS Process Builder to describe the activity coefficients in non-ideal mixtures. This model is especially useful for systems that exhibit strong deviations from the ideal behavior.

The activity coefficient γ_i for each component i in the liquid phase is given by:

$$\gamma_i = \exp\left(\frac{\sum_j \tau_{ij} x_j}{1 + \sum_j \tau_{ij} x_j} \right) \tag{2.24}$$

where: τ_{ij} is the binary interaction parameter between components i and j, x_j is the mole fraction of component j in the liquid phase.

The NRTL model provides a more accurate description of the phase behavior in non-ideal systems compared to models that assume ideal behavior, such as Raoult's law. This is particularly essential for the modeling of distillation systems in which deviations from ideality significantly impact separation performance [19], [14].

Table 2.1: Definitions of Variables Used in the Distillation Column Model

$\hat{V}_j$	Total volume of stage j [m^3]
$\bar{m}_{i,j}$	Volumetric mass holdup of component i on stage j [kg/m^3]
L_j	Mass flow rate of liquid leaving stage j [kg/s]
V_j	Mass flow rate of vapour leaving stage j [kg/s]
F_j^L	Mass flow rate of the liquid feed on stage j [kg/s]
F_j^V	Mass flow rate of the vapour feed on stage j [kg/s]
$S_{\text{frac},j}^L$	Fraction of the liquid mass flow rate leaving stage j via the liquid side-draw [-]
$S_{\text{frac},j}^V$	Fraction of the vapour mass flow rate leaving stage j via the vapour side-draw [-]
$x_{i,j}$	Mass fraction of component i in the liquid phase leaving stage j [kg/kg]
$y_{i,j}$	Mass fraction of component i in the vapour phase leaving stage j [kg/kg]
$x_{i,j}^L$	Mass fraction of component i in the liquid feed on stage j [kg/kg]
$y_{i,j}^V$	Mass fraction of component i in the vapour feed on stage j [kg/kg]
$\phi_{i,j}^L$	Fugacity coefficient of component i in the liquid phase leaving stage j [-]
$\phi_{i,j}^V$	Fugacity coefficient of component i in the vapour phase leaving stage j [-]
$\hat{u}_j$	Volumetric energy holdup [kJ/m^3]
h_j^L	Mass specific enthalpy of the liquid leaving stage j [kJ/kg]
h_j^V	Mass specific enthalpy of the vapour leaving stage j [kJ/kg]
h_L^F	Mass specific enthalpy of the liquid feed on stage j [kJ/kg]
h_V^F	Mass specific enthalpy of the vapour feed on stage j [kJ/kg]
M_{w_i}	Molecular weight of component i [kmol/kg]
M_i	Total mass of component i [kg]
M^L, M^V	Liquid and vapour phase total masses [kg]
x_i, y_i	Mass fractions in liquid and vapour phases [-]
ρ_L, ρ_V	Densities of liquid and vapour phases [kg/m^3]
$\hat{V}$	Total volume [m^3]
$\hat{u}$	Volumetric energy holdup [kJ/m^3]
$\bar{\boldsymbol{m}}$	Mass holdup vector [kg/m^3]
H	Enthalpy vector [kJ/kg]
P	Pressure [bar]
h^L, h^V	Specific enthalpies of liquid and vapour phases [kJ/kg]
M^T	Total mass on tray [kg]
$E_{M,i,j}^V$	Murphree component efficiency per tray [-]
$y_{\text{molar},i,j}$	Molar fraction of component i in vapour leaving stage j [mol/mol]
$y_{\text{molar},i,j}^*$	Molar fraction in equilibrium with liquid leaving stage j [mol/mol]

Chapter 3

Practical part

3.1 Description of the Distillation Column System

The UOP3CC Continuous Distillation Column is a self-contained unit designed for the continuous separation of binary mixtures. It consist of two main components: a floor-standing process unit and a bench-mounted control panel. The floor-standing frame consists of a welded tubular steel structure [12].

The primary separation task in this work for laboratory column is the separation of a methanol-water binary mixture. This mixture represents a common example in distillation studies due to its moderate deviation from ideality and its relevance in industrial applications. The goal is to achieve a methanol-rich distillate and a water-rich bottoms product, with the separation efficiency dependent on the operating parameters and column configuration [12].

The distillation column shown in Figure 3.1 itself is made of two glass sections, each with a diameter of 50 mm, and is configured for counter-current vapor-liquid operation. These sections are separated by a central feed point, where a liquid stream from the preheater is introduced and contain a total of eight sieve plates, divided evenly between the sections. Each plate is supported by a central rod and includes a weir and downcomer to maintain a liquid seal between stages. At the base of the column is the reboiler, constructed of stainless steel and equipped with a flame-proof immersion heater. During continuous operation, the reboiler circulates the product through a bottom product cooler. Vapor exiting the column is directed to a water-cooled shell-and-coil condenser. The condenser includes insulation to prevent heat exchange with the environment and is equipped with a pressure relief valve for safety. The flow of cooling water is controlled through a diaphragm valve, allowing temperature regulation.The system also features a glass decanter for the separation of immiscible liquid phases. In normal operation, the decanter is bypassed, allowing the condensate to flow directly to the reflux control valve or a product collection vessel [12].

Temperature monitoring is achieved through fourteen thermocouple sensors installed at strategic positions along the column, including the sieve plates, reboiler, feed, and condenser. The total pressure drop across the column is measured using automatic pressure sensors. [12].

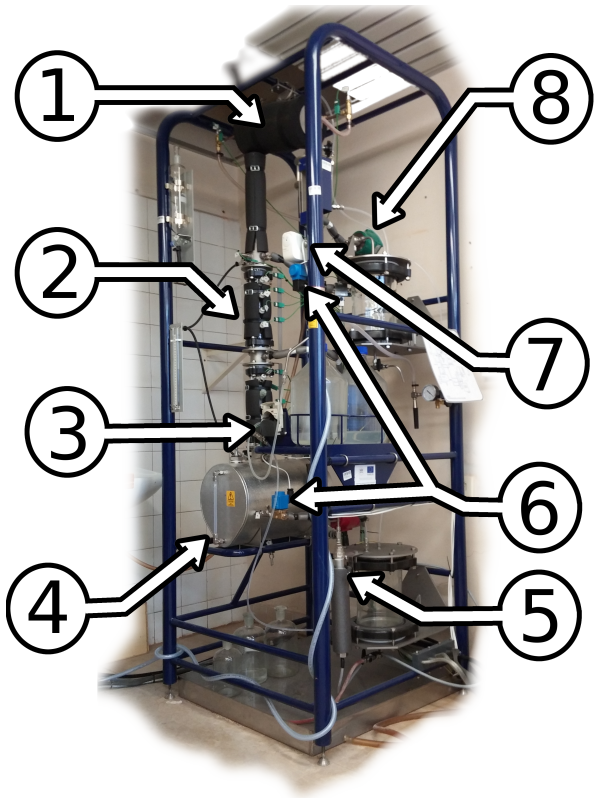

Figure 3.1: UOP3CC Column: 1. Condenser, 2. Column body, 3. Feed pump, 4. Reboiler, 5. Feed preheater, 6. Automatic valves, 7. Flow meter, 8. Reflux valve.

[24]

3.2 Feed and Waste Pump Calibration

In order to achieve a steady level in the reboiler, it is necessary to set the flow rate of the feed pump and the waste pump to the same value. That is why we decided to

perform a calibration on both pumps. For safety reasons, we only did the calibration with clean water. In our control simulation, we set a certain % of the flow rate in the range from 0-100 % and measured the volume that we managed to fill into the measuring cylinder per minute. The Table 3.1 and Figure 3.2 below summarize the values that we measured.

Table 3.1: Calibration data for feed pump and bot pump.

Feed Pump (%)	Feed Flow (ml/s)	Bot Pump (%)	Bot Flow (ml/s)
15	1.06	100	1.52
25	1.93	90	1.46
35	2.67	80	1.30
45	3.67	70	1.10
55	4.40	60	0.96
65	5.30		
75	6.00		
85	7.00		
95	8.10		

As shown in Table 3.1, the calibration for the bot pump was only performed for values from 60% to 100%, because below 60%, the flow rate of the bot pump is very small compared to the feed pump, so it was ineffective and time consuming to measure below this value. After processing the data, we obtained the following dependencies:

$$\text{Feed pump:} \quad y = 0.09x - 0.28 \tag{3.1}$$

$$\text{Bottom pump:} \quad y = 0.01x + 0.08 \tag{3.2}$$

The pump power settings for both pumps were selected to ensure a steady liquid level in the reboiler. Specifically, the feed pump was set to 21% and the bottom pump to 78% of their power. A comparison of measured and estimated data is shown in Figure 3.2, where it is shown that the measured data match the estimated data.

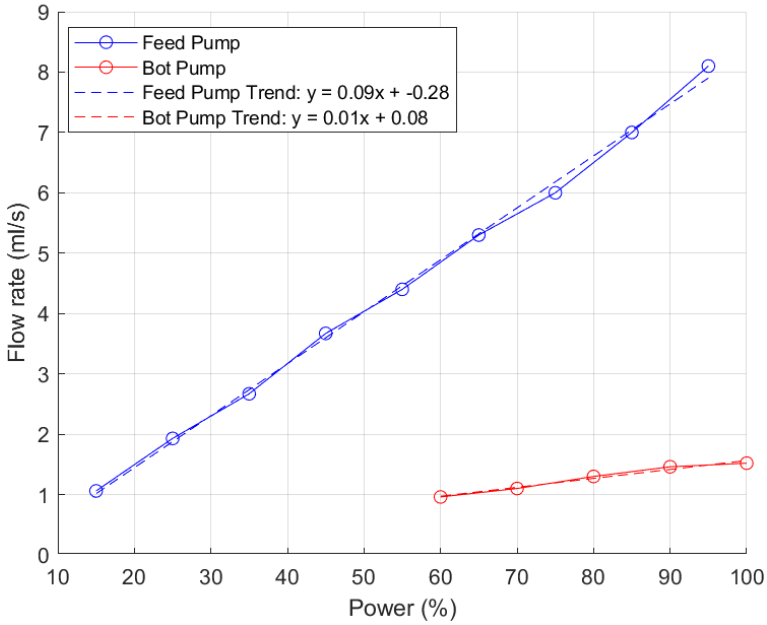

Figure 3.2: Calibration curve for feed and waste Pump.

3.3 Modeling of the Distillation Column in AVEVA

In this section, the process of modeling the distillation column for the methanol-water mixture is described in AVEVA Process Simulation software. The aim of this model was to replicate the behavior of a real distillation column under steady-state operating conditions. This approach is useful for comparing the behavior of a real column with simulations, and also with correct model, we can estimate parameters that we cannot measure on a real device like reflux flow or duty of condenser, which is necessary for calculating of flow cooling water.

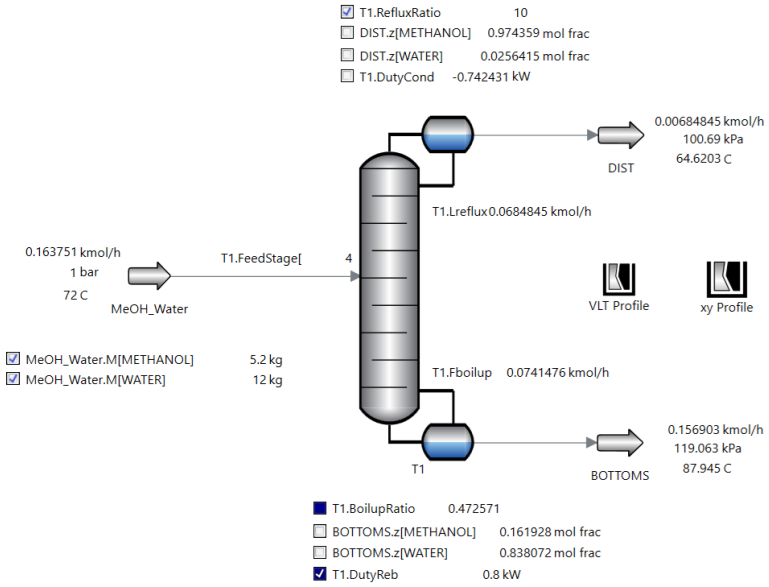

Figure 3.3: Simulation environment AVEVA.

3.3.1 Model Setup

The drag-and-drop functionality of AVEVA Process Simulation was used to construct the distillation column model. At the same time, we worked on operating the laboratory column and tuning the input parameters, which helped us set the input parameters in such a way as to get as close as possible to the behavior of the real column. The key parameters for the model were configured as follows:

Table 3.2: Key Parameters of the Distillation Column Model in AVEVA

Parameter	**Value**	**Units**
Feed Composition	Methanol (0.6655), Water (0.3345)	mol/mol
Feed Flow Rate	0.1638	kmol/h
Feed Temperature	72	°C
Feed Pressure	101 325	Pa
Number of Stages	8	–
Feed Stage	4th (from top)	–
Column Pressure	101 325	Pa
Reboiler Duty	0.8	kW
Tray Height	100	mm
Column Height	800	mm

The distillation column model provided an estimate of the heat duty of the condenser Q_{cond}. We choose to heat the cooling water approximately by 5 °C. An increase of approximately 5 °C in the temperature of the cooling water is commonly chosen in the condenser design as a compromise between the size of the heat exchanger, the consumption of the cooling water and the efficiency of the heat transfer. Consequently, it was possible to calculate the required cooling water volume flow rate using the following energy balance equation:

$$\dot{m}_{\text{w}} = \frac{|Q_{\text{cond}}|}{c_p \cdot \Delta T} = \frac{742.431}{4180 \cdot 5} = \frac{742.431}{20,900} \approx 0.0332\,\text{kg/s} \tag{3.3}$$

where $\dot{m}_{\text{w}}$ is the mass flow rate of the cooling water, $|Q_{\text{cond}}|$ is the absolute value of the condenser heat duty, c_p is the specific heat capacity of the water and ΔT is the temperature difference.

Now, the volumetric flow rate can be calculated using the density of water $\rho = 1000\,\text{kg/m}^3$:

$$\dot{V} = \frac{\dot{m}_{\text{w}}}{\rho} = \frac{0.0332}{1000} = 0.0000332\,\text{m}^3/\text{s} = 0.0332\,\text{L/s} \tag{3.4}$$

Converting to liters per minute (L/min):

$$0.0332\,\mathrm{L/s} \times 60 = 1.992\,\mathrm{L/min} \tag{3.5}$$

Our flow meter measures the flow rate in units of CG/min (centigrams per minute):

$$0.0332\,\mathrm{kg/s} \times 100,000 = 3320\,\mathrm{CG/min} \tag{3.6}$$

3.4 Modeling of the Distillation Column in gPROMS Process Builder

The gPROMS Process Builder software was utilized to model the distillation column for the methanol-water system. This section provides a detailed description of the modeling process, divided into two subsections. The first subsection describes the creation of a simplified shortcut model to familiarize ourself with the environment, and the second subsection focuses on a more complex model.

3.4.1 Shortcut gPROMS Model

As an initial step, a simplified distillation model was implemented in the gPROMS modeling environment. The purpose of this was not to obtain precise simulation results, but rather to become familiar with the software interface, modeling workflow, and result visualization tools offered by gPROMS. At this stage, no detailed thermodynamic models or column hydraulics were considered.

Table 3.3: Input Feed Parameters

Parameter	**Value**	**Units**
Feed temperature	72	°C
Feed pressure	101,325	Pa
Molar composition (Water)	0.3345	–
Molar composition (Methanol)	0.6655	–
Total feed flow rate	0.1638	kmol/h

Table 3.4: Column Setup Parameters

Parameter	Value	Units
Condenser type	Total	–
Methanol molar fraction in bottom	0.4954	–
Water molar fraction in distillate	0.05	–
Number of stages	8	–
Condenser pressure	101.325	Pa
Reboiler pressure	1.3	kPa
Shortcut method	Fenske's method	–

Table 3.5: Model Output Results

Parameter	Value	Units
Reflux ratio	0.7172	–
Feed stage from the top	2.13994	–
Boilup ratio	0.094	–
Condenser temperature	64.48	°C
Reboiler temperature	79.109	°C
Reboiler duty	0.1305	kJ/s
Condenser duty	-0.3283	kJ/s

These output parameters shown in Table 3.5 do not match the laboratory column parameters and this model does not accurately describe the behavior of a laboratory distillation column mainly because it is not possible to include the column design parameters.

3.4.2 Detailed gPROMS Model

In the next stage, a more complex drag-and-drop model was constructed to better represent the laboratory distillation column. This model includes additional parameters and features to more accurately simulate the real system. For the column, the model allowed for a comprehensive input of geometric and operational parameters. We either found the design parameters in the manual for the column or manually measured then on the device.

- **Column geometry:** Specifications for the height, diameter and number of stages of the column.

- **Reflux drum design:** Configuration of the drum to control the reflux flow.
- **Reboiler design:** Design details for the reboiler, including duty and hydraulics.
- **Tray design:** include parameters such as tray spacing, active and hole area fractions, hole diameter, weir height and length
- **Pressure profile:** Definition of the pressure drop across the column.
- **Hydraulics of the condenser and reboiler:** Detailed modeling of fluid flow in these units.
- **Initial guess and numerics:** Settings for starting values and numerical solvers to ensure convergence of the simulation.

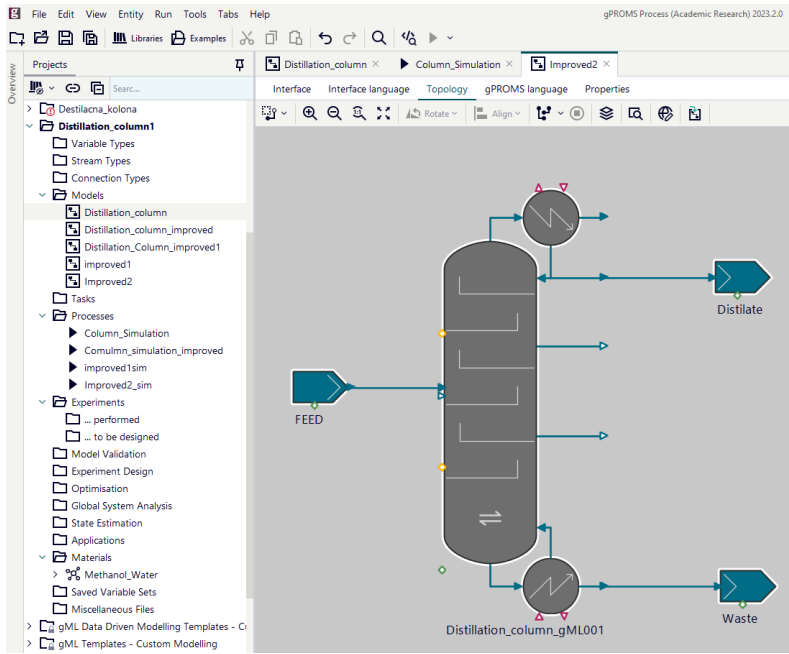

Figure 3.4: gPROMS environment with detailed model.

This detailed model provided a more accurate and flexible simulation of the laboratory column than the shortcut model, enabling the analysis of dynamic and steady-state behavior under various operating conditions. This model was mainly used to compare the column behavior with the AVEVA model, which is described in the following subsection.

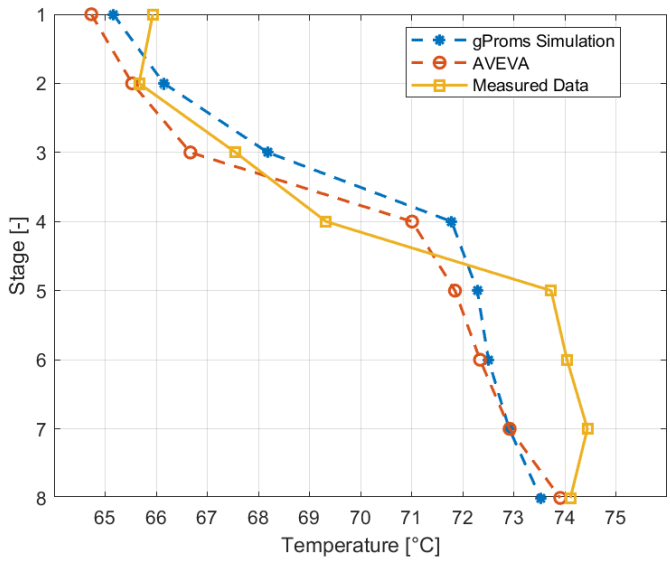

Figure 3.5: gPROMS Environment with Shortcut Model.

3.4.3 Detailed gPROMS and AVEVA Model with Laboratory Column Temperature Profile Comparison

As shown in Figure 3.5 gPROMS simulation and the AVEVA simulation have similar temperature profiles. There is a 1 °C difference in the fourth and fifth stages, which can be caused by different input parameters of each model. For example, gPROMS software has more options for column design than AVEVA. When comparing the temperature profile of the real column with gPROMS and AVEVA simulation, the temperatures at the top of the column are closely aligned. However, differences are observed at the feed stage. The temperature in the laboratory column is lower, which could be caused by damaged or ineffective isolation, leading to undesired heat transfer around the feed stage. Also, ambient temperature is not involved in the model. Similarly, differences are evident at the bottom of the column. These deviations could also be attributed to a column design, as there is a long part above the first stage, nearly as long as the entire column itself. The temperature signals are also noisy, and a representative temperature for each stage had to be chosen as an average value, which could also cause mismatch. In the laboratory column, the temperature in the eighth stage should be higher than in the seventh stage, but it was a lower value. Where the reboiler connects to the column, the foam insulation does not adhere properly due to the column's expansion at that point or maintenance of the temperature sensor should

also be necessary.

3.5 Data-Driven Building of State-Space Model

Before implementing any control strategy for the distillation column, a dynamic model of the process must be identified to represent how the system responds over time. In this section, we would like to show how I identified and simulated a state-space model using data that I experimentally measured on a real device for the design of PI controller and an advanced LQR control.

To design a discrete PI controller and discrete linear quadratic regulator capable of transitioning at least between two steady states of the distillation column, an experiment was performed to identify the system dynamics around selected operating conditions. In Table 3.6 the following steps summarize the changes in the manipulated variables during the experiment:

Table 3.6: Summary of the experimental steps for operating point identification

Time [s]	**Reflux [%]**	**Reboiler Duty [kW]**	**Description**
0	90	0.8	Initial steady state
1452	70	0.8	Step decrease in reflux
2424	70	0.85	Step increase in reboiler duty

I then processed the data in the Matlab environment, using the N4SID (Numerical Subspace State Space System IDentification) function. This method identifies a model from measured input-output data using singular decomposition. In Figure 3.6 and matrices below I would like to expres the state-space model.

$$\begin{bmatrix} x_1[k+1] \\ x_2[k+1] \\ x_3[k+1] \\ x_4[k+1] \end{bmatrix} = \begin{bmatrix} 0.9675 & -0.0065 & -0.0015 & -0.0244 \\ 0.0065 & 0.9297 & -0.0216 & -0.0532 \\ 0.0075 & 0.0390 & -0.6778 & 0.7106 \\ 0.0202 & -0.0460 & -0.7008 & -0.5507 \end{bmatrix} \begin{bmatrix} x_1[k] \\ x_2[k] \\ x_3[k] \\ x_4[k] \end{bmatrix} + \begin{bmatrix} -0.0716 & 0.0003 \\ 0.1254 & -0.0000 \\ 1.0048 & 0.0051 \\ 2.7444 & -0.0063 \end{bmatrix} \begin{bmatrix} u_1[k] \\ u_2[k] \end{bmatrix}$$

$$\begin{bmatrix} y_1[k] \\ y_2[k] \end{bmatrix} = \begin{bmatrix} -14.7359 & 0.4218 & -0.6222 & -0.4708 \\ -1.7205 & -1.7629 & -0.1106 & 0.1150 \end{bmatrix} \begin{bmatrix} x_1[k] \\ x_2[k] \\ x_3[k] \\ x_4[k] \end{bmatrix} + \begin{bmatrix} 0 & 0 \\ 0 & 0 \end{bmatrix} \begin{bmatrix} u_1[k] \\ u_2[k] \end{bmatrix}$$

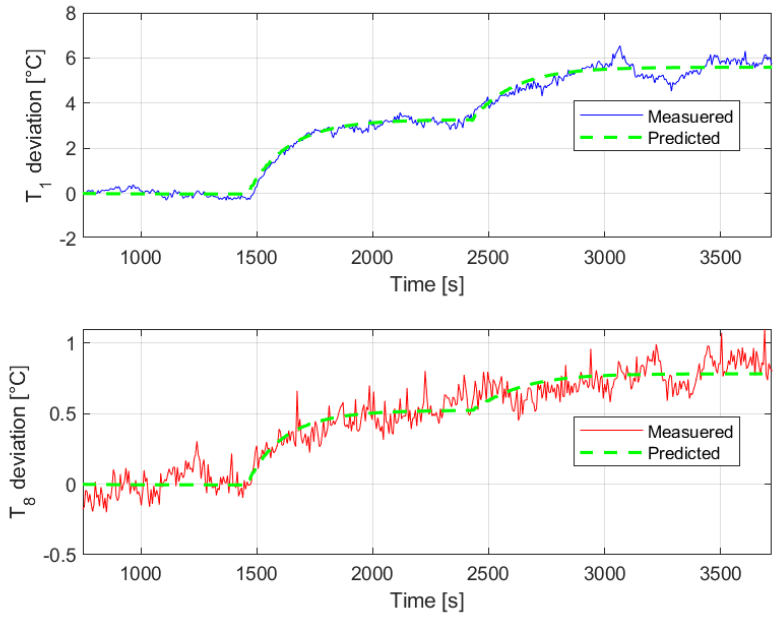

Figure 3.6: Output data with identified state-space model.

In Figure 3.6, the identification results are presented that illustrate the ability of the model to predict the temperature deviations in a distillation column. The prediction aligns very well with the measured response across the entire time interval, successfully capturing both the dynamics and steady-state behavior.

To determine the accuracy of the model's prediction, I used the RMSE metric. which is described below:

$$\text{RMSE} = \sqrt{\frac{1}{n}\sum_{i=1}^{n}(y_i - \hat{y}_i)^2} \tag{3.7}$$

where n is the number of observations, y_i is the actual value for the i-th observation and $\hat{y}_i$ is the predicted value for the i-th observation.

Values of RMSE are T_1: 0.2685 °C, T_8: 0.0977 °C.

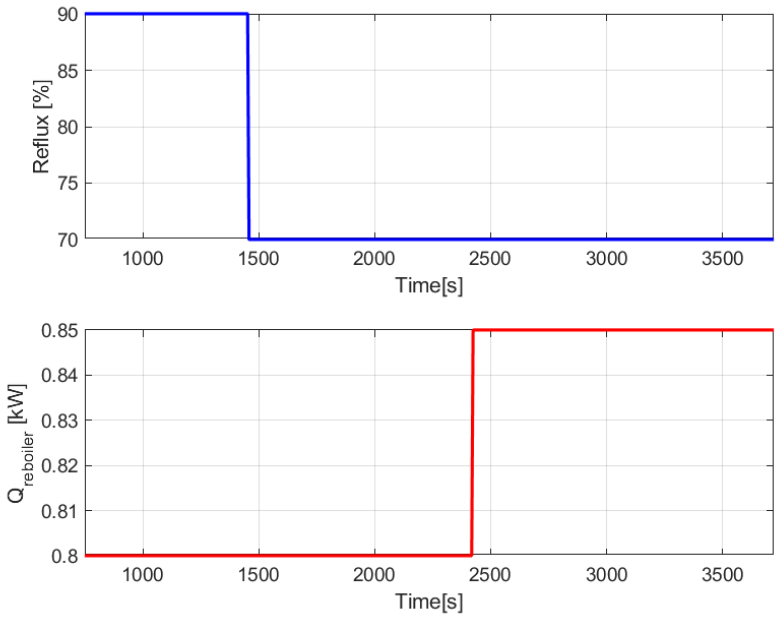

Figure 3.7: Input Data.

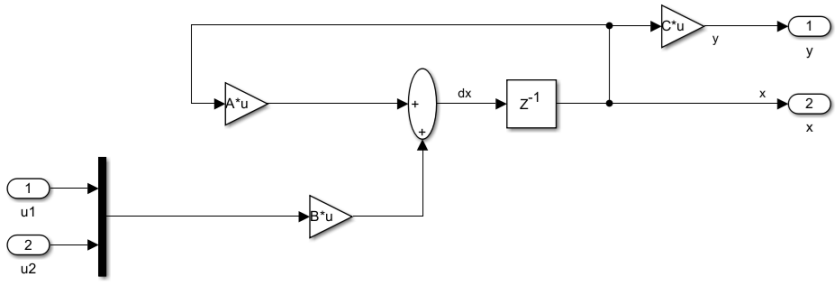

Figure 3.8: Scheme of discrete linear model in Simulink.

3.6 PI Temperature Control in the Distillation Column

In this section, the temperature control strategy for the distillation column is described, where a closed-loop PI control system was implemented. The step changes were performed from a steady-state condition, where the temperature T_8 was 76.01 °C and T_1 was 65.3 °C."

3.6.1 Temperature Control at the Top of the Column T_1

The temperature at the top of the column T_1 is controlled by adjusting the reflux flow rate. The reference for the control system is the setpoint temperature at the column head, which is 70.3 °C, while the measured temperature from the sensor provides the feedback. The PI controller adjusts the reflux flow to minimize the difference between the desired and actual temperature.

3.6.2 Temperature Control at the Bottom Tray T_8

For the temperature control in the bottom tray T_8, the duty of the reboiler is manipulated. The reference for this control loop is the desired temperature in the bottom tray, which is 76.81°C, and the measured temperature is a feedback to the controller. The PI controller adjusts the power input to the reboiler, controlling its duty in kW to maintain the temperature at the desired setpoint.

I chose a setpoint of 70.3 ° C and 76.81 ° C as the step changes values from steady

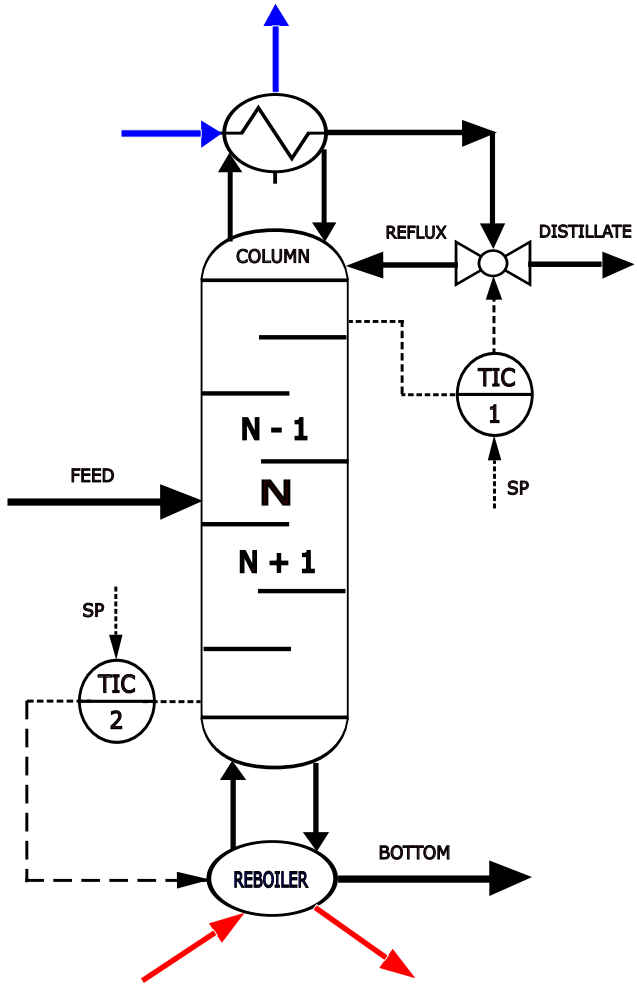

Figure 3.9: LV configuration of distillation column.

states according to the identification. A larger temperature change could cause the reboiler to want to deliver a large amount of energy to the system and cause the column stage to flood, or conversely, at a lower temperature, cause the stage to dry out. Operating too far from the setpoint can disrupt the steady state of the column, leading to reduced separation efficiency or process instability.

3.7 Tuning PI Controllers

The PI controllers for the distillation column were tuned using the Skogestad method, which is a widely used approach for controller tuning based on process transfer functions. This method allows for efficient calculation of the proportional gain (K_p) and the integral time (T_i) for the PI controllers.

First, the transfer functions between the controlled variables (temperatures) and the manipulated variables (reboiler duty and reflux flow rate) were derived. These transfer functions were obtained by transforming the state space model into a transfer function using the ss2tf functionality in MATLAB.

For the bottom tray temperature (T_8) and the reboiler duty (Q), the transfer function was obtained as:

$$G(s) = \frac{T_8(s)}{Q(s)} = \frac{5.16}{6.123s + 1} \tag{3.8}$$

$$G(s) = \frac{T_1(s)}{R(s)} = \frac{-0.1651}{13.53s + 1} \tag{3.9}$$

3.7.1 Calculation of the PI Controller Parameters and Control Performace

Once the transfer functions were obtained, the Skogestad method was applied to calculate the controller parameters, namely the proportional gain (K_p) and the integral time (T_i) for the temperature control loops of the bottom and top tray.

The proportional gain (K_p) and the integral time (T_i) are given by the following equations:

$$K_p = \frac{T}{K} \cdot (T_c + d) \tag{3.10}$$

$$T_i = \min\left(T,\ 4 \cdot (T_c + T_d)\right) \tag{3.11}$$

where T is the process time constant, K is the steady-state gain of the transfer function, T_c is the closed-loop time constant and T_d is the system time delay and d and represents the apparent or effective delay of the process, accounting for any additional delay or unmodeled dynamics.

These equations allow for the determination of the PI controller parameters based on the process dynamics described by the transfer functions. The closed-loop time constant (T_c) and the time delay (T_d) were estimated from the dynamics of the process [21]. The calculated parameter for the control of the reboiler duty was $K_p = 0.006$ and $K_i = 0.007229$ and for the control of reflux was $K_p = -9.7295$ $K_i = -0.0874$.

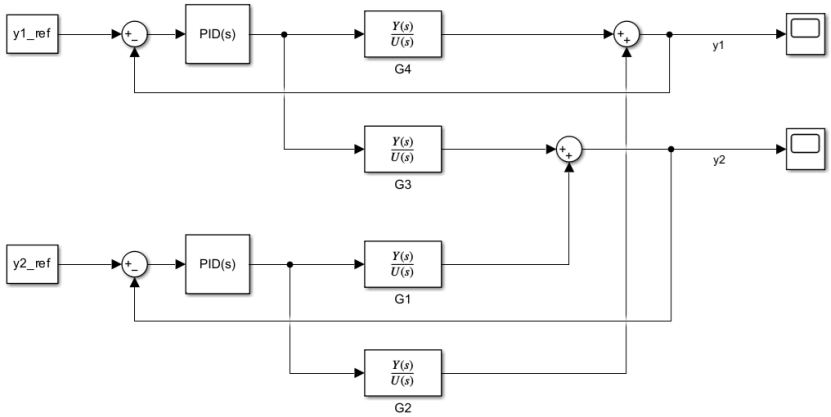

Figure 3.10: Block diagram of PID control in Simulink.

In Figures 3.11 and 3.12 simulated reference tracking of temperature T_1 and T_8 is shown. Both temperatures reach the setpoint around the time 400 seconds with a small overshot in temperature T_8. Control action reflux drops by almost 50% almost immediately and then oscillates for about 200 seconds and reaches a steady value after 600 seconds. In the early part of the response, both control signals show a noticeable "toothed" pattern. This might be due to interactions between the two PI controllers,

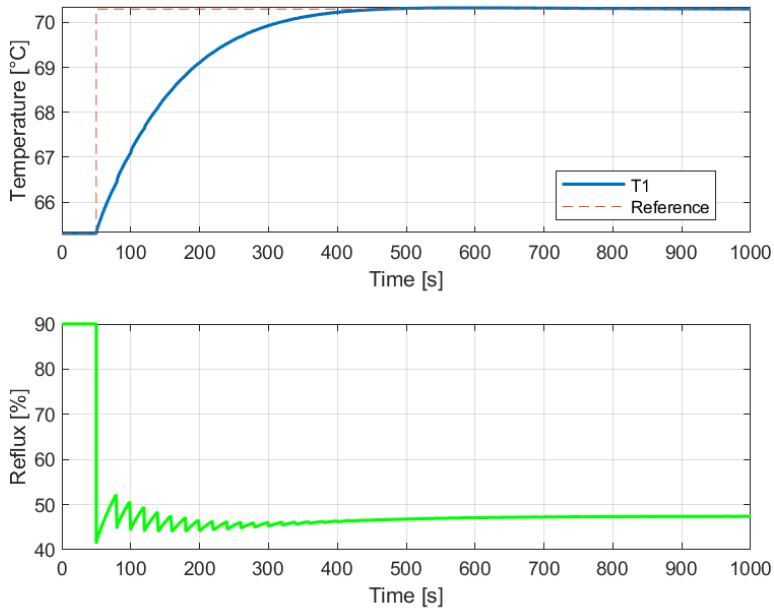

Figure 3.11: Simulated Temperature of T1 (top of the column) with the setpoint (top) and the control action (bottom) of the reflux valve.

since the system is MIMO and the control loops can affect each other. Since this behavior did not appear in the experimental data, it is likely related to the simulation setup. The control action duty of the reboiler has a smoother response with a small overshoot around 200 seconds and then stabilizes around 900 seconds. The controller reached a steady-state consistent with the behavior observed during the identification phase. After simulation of PI controllers, the controllers were tested in the laboratory distillation column system to verify their performance.

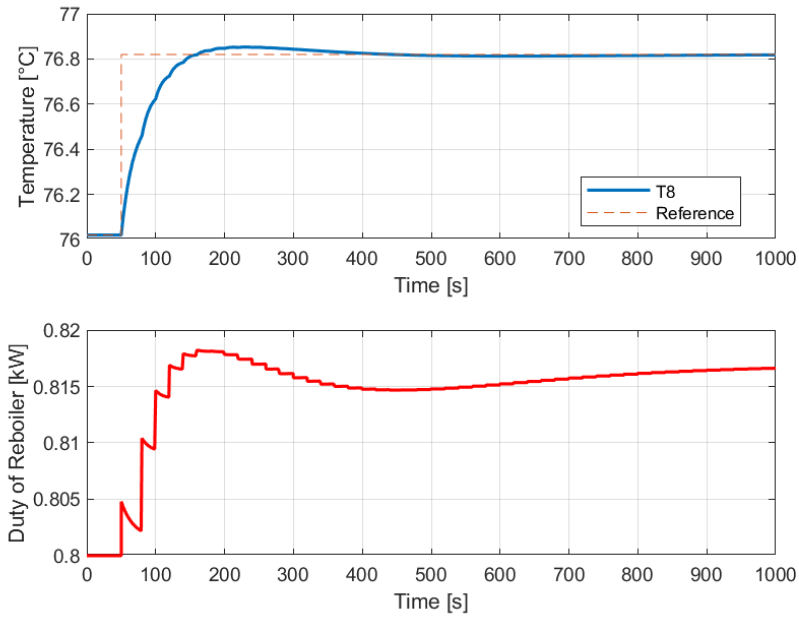

Figure 3.12: Simulated Temperature of T8 (bottom tray) with the setpoint (top) and the control action (bottom) of the reboiler duty.

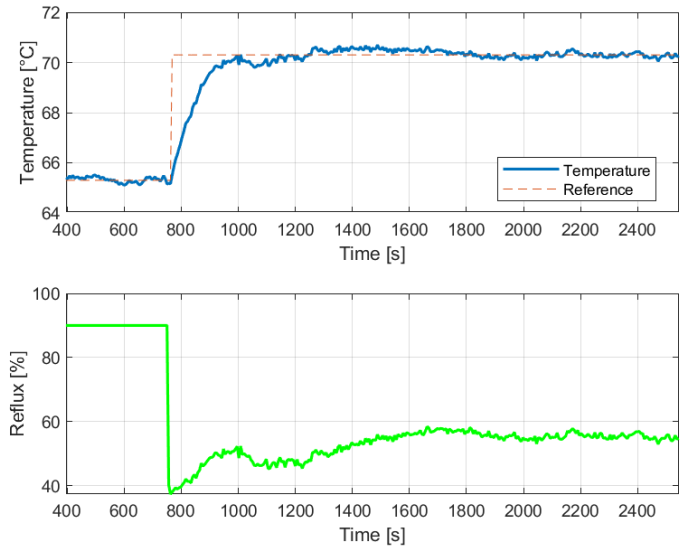

Figure 3.13: Temperature of T1 (top of the column) with the setpoint (top) and the control action (bottom) of the reflux valve.

In figures 3.13 and 3.14 we can see the time dependence of the output variables, the temperature T_1 at the top of the column, and the temperature T_8 at the bottom. Below the graphs are shown the control actions, namely the reboiler duty, which has a greater influence on the temperature T_8 and the percentage of opening the valve for return flow into the column (reflux) with greater influence on T_1. At control of temperature T_1 in the initial increase, the reflux reaches 40% relatively quickly, indicating that the controller is trying to reach its setpoint as quickly as possible. The temperature T_1 reaches its set point around 1200 seconds and then stays around the set point without overshot. The controller reached a steady state consistent with the behavior observed during the identification phase.

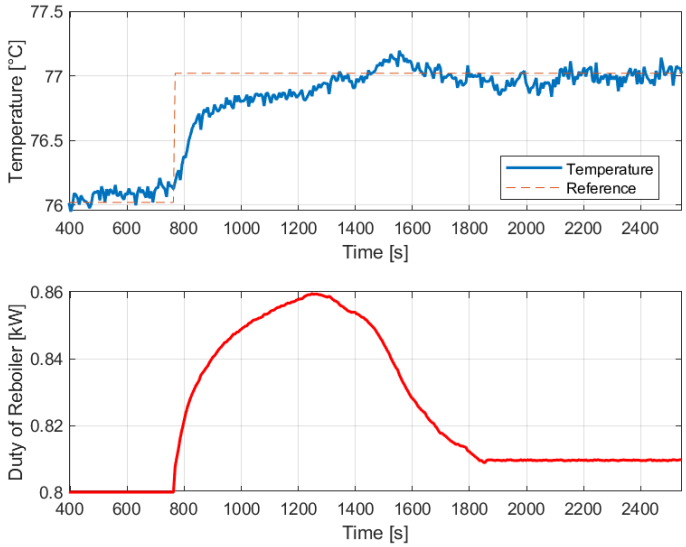

Figure 3.14: Temperature of T8 (bottom tray) with the setpoint (top) and the control action (bottom) of the reboiler duty.

At temperature T_8, a similar behavior is visible as at temperature T_1. When the controller starts up, we see an overshoot in the control action at the beginning, which is also visible at temperature T_8 at a time of around 1500 seconds. In contrast to reflux, the duty of the reboiler subsequently stabilizes at a time of around 1800 seconds. However, what is interesting is that the temperature of T_8 oscillates more than T_1. This may be due to the fact that the duty of reboiler has a greater influence on whole system than reflux, so even a small change in the duty of reboiler can cause larger

oscillations at temperature T_8. The behavior of the temperatures and control actions in the laboratory column are similar to those in simulation. The differences from simulation are in the duty of the reboiler, because in the laboratory column we got around 0.4 kW higher overshoot and reflux in the laboratory column stabilized over 20% higher, but the temperature behavior matches simulation. Overshooting in the control action duty of a reboiler would cost money in energy in industrial practice, and fast changes in reflux could damage the valve over time. Therefore, it would be appropriate to design a more advanced control for such a system.

3.8 Linear Quadratic Regulator Design

While PID control provides satisfactory performance, it lacks the ability to handle multivariable systems. Therefore, this chapter presents the implementation of a linear quadratic regulator for improved performance. Firstly we calculated the matrices K_x and K_i mentioned in the theoretical part using the Matlab environment and especially the dlqr routine, which requires as input the linear system matrices A, B and the weighting matrices defined as:

- Q_i, penalizing the integral error (temperature tracking),
- Q_t, combining the state and integrator weights,
- Q_u, the input weight matrix.

In our case, it was necessary to change the input matrix Q_u, especially the first row and the first column with a value of 100,000, because otherwise the control action of the reboiler would be very aggressive. We also adjusted the reflux weight with a value of 4 so that there would be no significant undershoot in the control action. I found these values using simulation by changing them and observing the behavior of the system [18].

$$Q_i = \begin{bmatrix} 1 & 0 \\ 0 & 1 \end{bmatrix} \tag{3.12}$$

$$Q_t = \begin{bmatrix} 1 & 0 & 0 & 0 & 0 & 0 \\ 0 & 1 & 0 & 0 & 0 & 0 \\ 0 & 0 & 1 & 0 & 0 & 0 \\ 0 & 0 & 0 & 1 & 0 & 0 \\ 0 & 0 & 0 & 0 & 1 & 0 \\ 0 & 0 & 0 & 0 & 0 & 1 \end{bmatrix} \tag{3.13}$$

$$Q_u = \begin{bmatrix} 100000 & 0 \\ 0 & 4 \end{bmatrix} \tag{3.14}$$

The values K_x and K_i are presented below:

$$K_x = \begin{bmatrix} -0.6871 & 0.1390 & -0.0036 & 0.0025 \\ 169.7654 & 19.2498 & 1.0612 & -2.5730 \end{bmatrix}$$

$$K_i = \begin{bmatrix} -0.0007 & 0.0006 \\ 0.1491 & 0.2002 \end{bmatrix}$$

3.8.1 State Observer Design

System identification revealed that a state-space model with four states provides the best fit for the two-input, two-output system. In addition to the output temperatures, there are other parameters that affect the behavior of the process. In order to be able to estimate these parameters well, we decided to design a discrete state observer for the LQR controller [18].

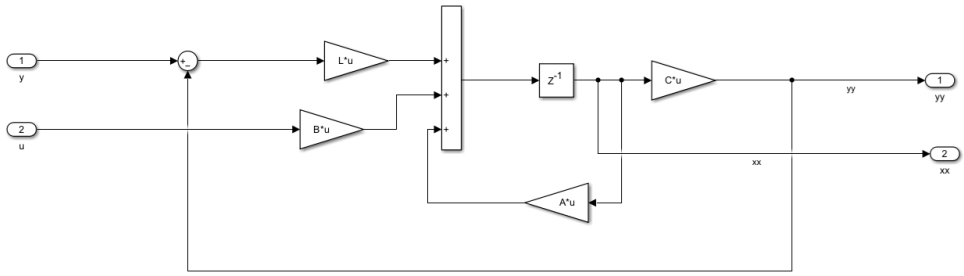

Figure 3.15: Scheme of discrete state observer.

In the Matlab environment, I calculated the observer gain matrix using dlqe (Discrete Linear Quadratic Estimator) which requires as inputs matrices of linear system A, C and the following weighting matrices:

- G, the identity matrix, assuming full process noise distribution,
- Q_e, representing confidence in the model (process noise covariance),
- R_e, representing confidence in the measurements (measurement noise covariance).

We did not adjust the values of these matrices, as the state observer was effective even without adjustment [18].

$$G = \begin{bmatrix} 1 & 0 & 0 & 0 \\ 0 & 1 & 0 & 0 \\ 0 & 0 & 1 & 0 \\ 0 & 0 & 0 & 1 \end{bmatrix} \tag{3.15}$$

$$Q_e = \begin{bmatrix} 1 & 0 & 0 & 0 \\ 0 & 1 & 0 & 0 \\ 0 & 0 & 1 & 0 \\ 0 & 0 & 0 & 1 \end{bmatrix} \tag{3.16}$$

$$R_e = \begin{bmatrix} 1 & 0 \\ 0 & 1 \end{bmatrix} \tag{3.17}$$

The Kalman gain L_K was first calculated using:

$$L_K = \texttt{dlqe}(A, G, C, Q_e, R_e)$$

Then, the observer gain matrix L was computed as:

$$L = A \cdot L_K$$

This procedure is used to estimate the system states in the presence of noise and measurement inaccuracies.

$$L = \begin{bmatrix} -0.0610 & -0.0150 \\ 0.0467 & -0.4030 \\ -0.0349 & 0.1641 \\ 0.0296 & 0.0021 \end{bmatrix}$$

As a check of the correctness of the calculation of the observer parameters, I simulated the states and outputs with the observed ones. In Figure 3.16 we can see the comparison. It is clear from the legend that we are plotting eight states. Since we see only four dependencies in Figure 3.16, this means that the observer parameters were calculated correctly and that the observed states and outputs match the simulated ones.

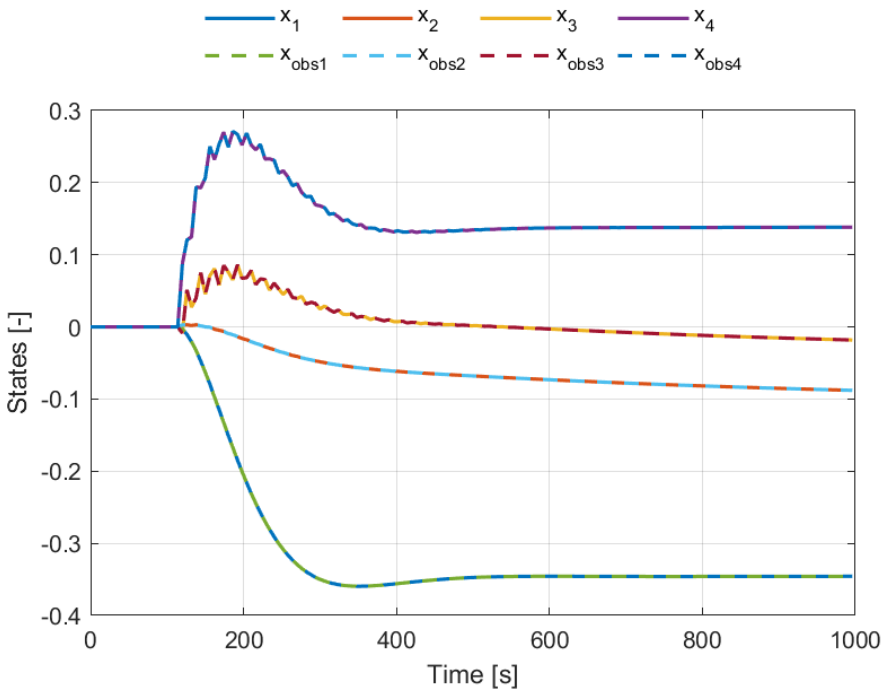

Figure 3.16: Comparing of simulated states with observed states.

In Figure 3.17 the observed outputs are shown compared to the simulated, where y_1 represents the temperature at the bottom of the column T_8 and y_2 the temperature at the top T_1. The temperature T_8 stabilizes after approximately 300 seconds while the temperature T_1 stabilizes after approximately 500 seconds with a small overshoot. As in 3.16, we can see that the observed outputs match the system outputs. This behavior indicates that the observer is able to reconstruct the states of the system accurately over time. The results validate that the observer dynamics is well tuned, and the model used is adequate for capturing the system behavior.

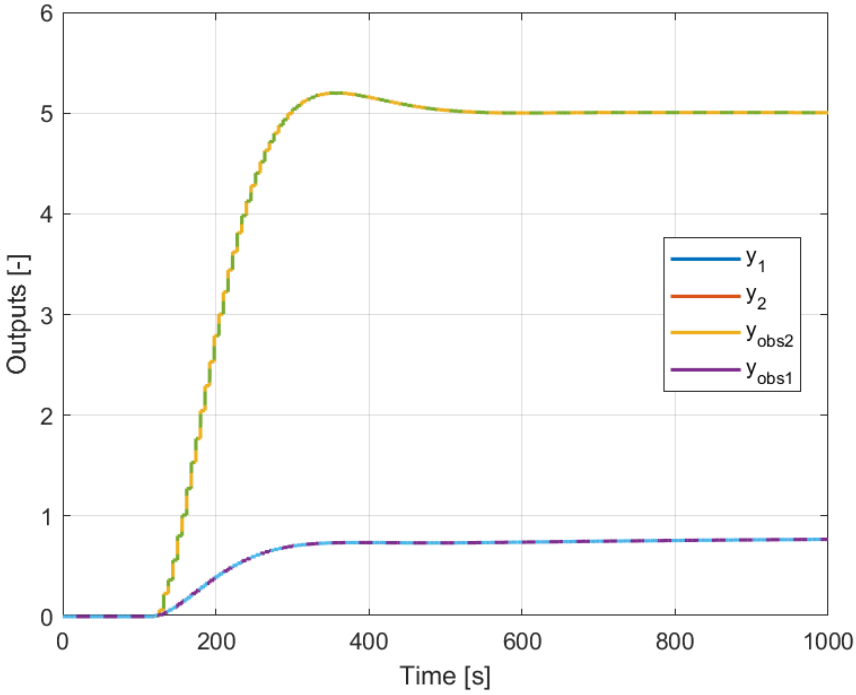

Figure 3.17: Comparing of simulated outputs with observed outputs.

In the next step, I created a Simulink scheme, where I connected my identified process with the LQR control and state observer. I also implemented anti-windup in the scheme using the back-calculation method due to saturation and integral part of the LQR controller. The complete scheme is shown in Figure 3.18.

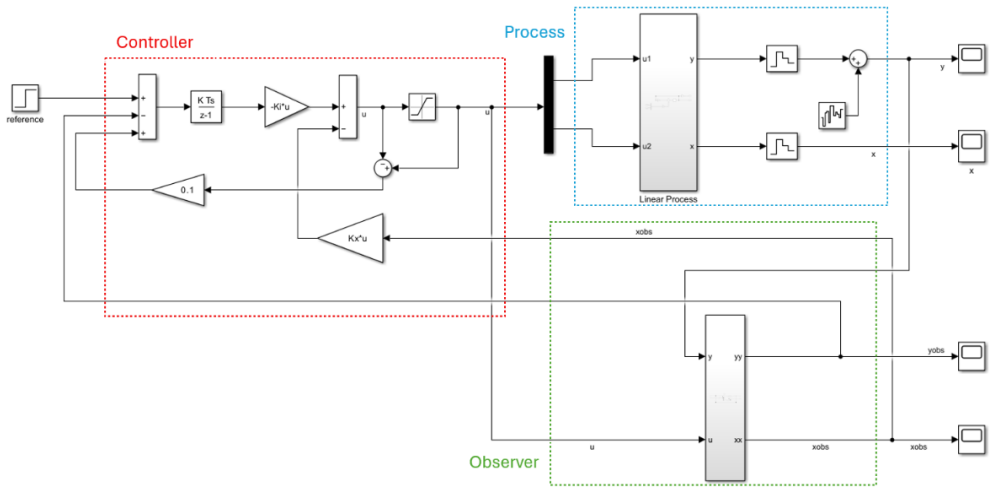

Figure 3.18: Control scheme with LQR controller and state observer.

The control loop begins with the reference input, representing the desired change value of the controlled output. This reference is then processed through block that incorporates an integrator to ensure accurate tracking and eliminate steady-state error with integration. The resulting signal is used to compute the control action together with the estimated states multiplied with feedback gain matrix. The central part of the scheme is the block labeled Linear Process, which represents the plant model in discrete-time state-space form. The plant receives the control input and provides the system output as well as the internal states. To reconstruct the unmeasured states, a state observer is implemented. It uses the input and output of the plant to estimate the internal states and outputs of the system. These estimates are then sent back into the LQR controller, which calculates the control signal. Throughout the model, data logging blocks are placed at various points to record the time dependence during simulation. These signals are used for post-processing and evaluation of the controller performance.

3.8.2 Control performance of LQR Controller

The Figures 3.19 and 3.20 show the performance of the LQR controller in simulation, where the objective is to regulate the top and bottom temperatures by manipulating the reflux and reboiler duty.

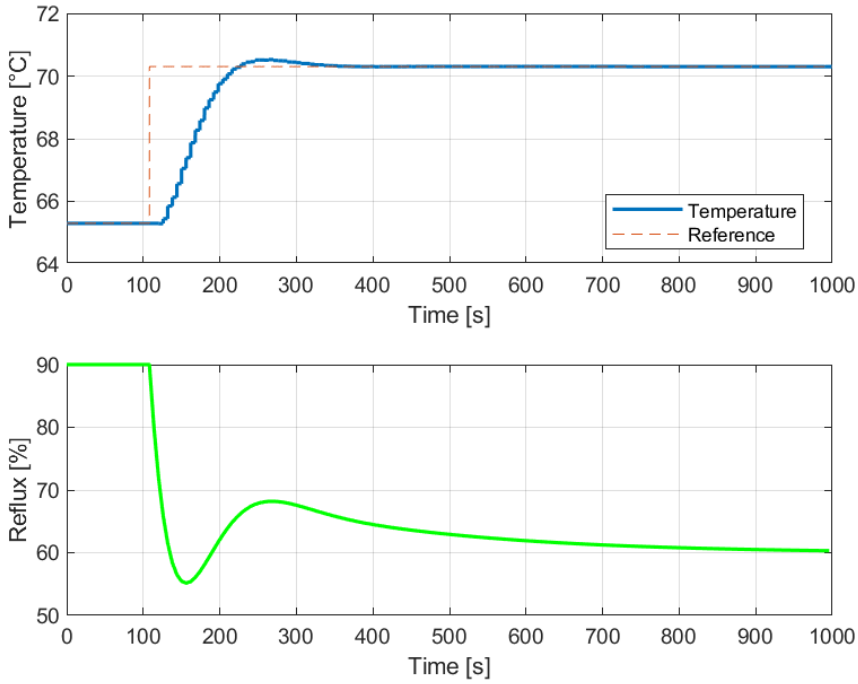

Figure 3.19: Simulated reference tracking of temperature on the top of column (top) with input signal (bot).

The temperature on the top of the column T_1 follows the reference trajectory with a smooth response, reaching the setpoint around 350 seconds with minimal overshoot. Reflux stabilize around time 900 seconds, while there is a slight undershoot around 150 seconds in the control action, but we got rid of the oscillations that occurred in the simulations with PI control. Compared to the PI simulated controller, the change in reflux is smoother and less aggressive, both in terms of rate and amplitude.

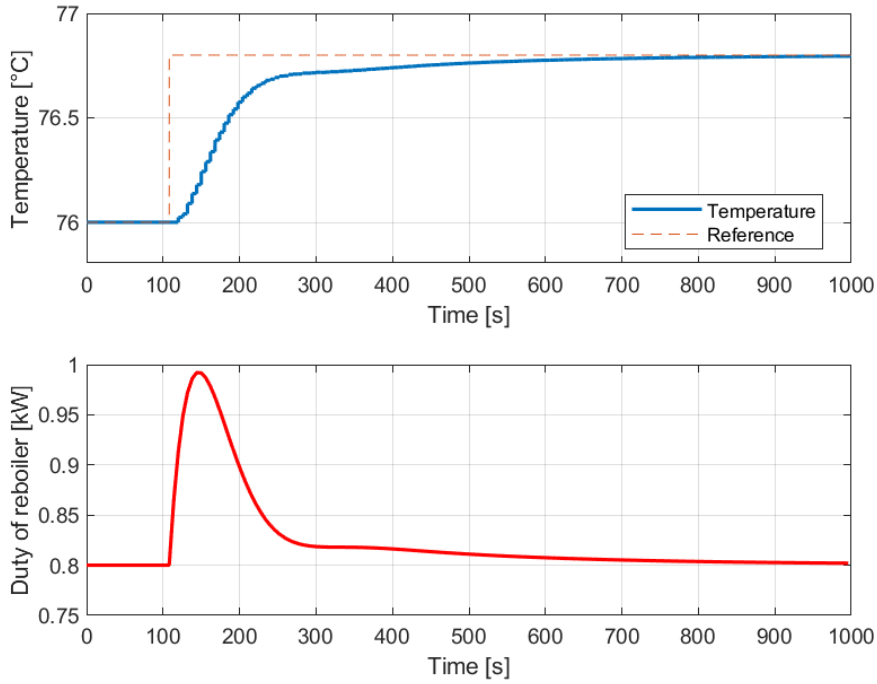

Figure 3.20: Simulated reference tracking of temperature on the bottom of column (top) with input signal (bot).

The temperature in the bottom controller T_8 also successfully follows the reference with a longer settling time of around 800 seconds. We do not see any overshoot in the temperature, even though it occurs with the duty of reboiler, which is even larger than with the PI controller simulation. This could also be caused by the influence of reflux, since with LQR control the inputs can coordinate together. I had to adjust the controler using the weight matrix of the inputs Q_u, where I had to penalize the reboiler duty with a value of up to 100,000 and the reflux with only a value of 4. This penalty was necessary because the reflux ranges from 0 - 1.75 and the reflux ranges from 0 - 100. If we had not adjusted the weights, the duty of reboiler would have been more aggressive.

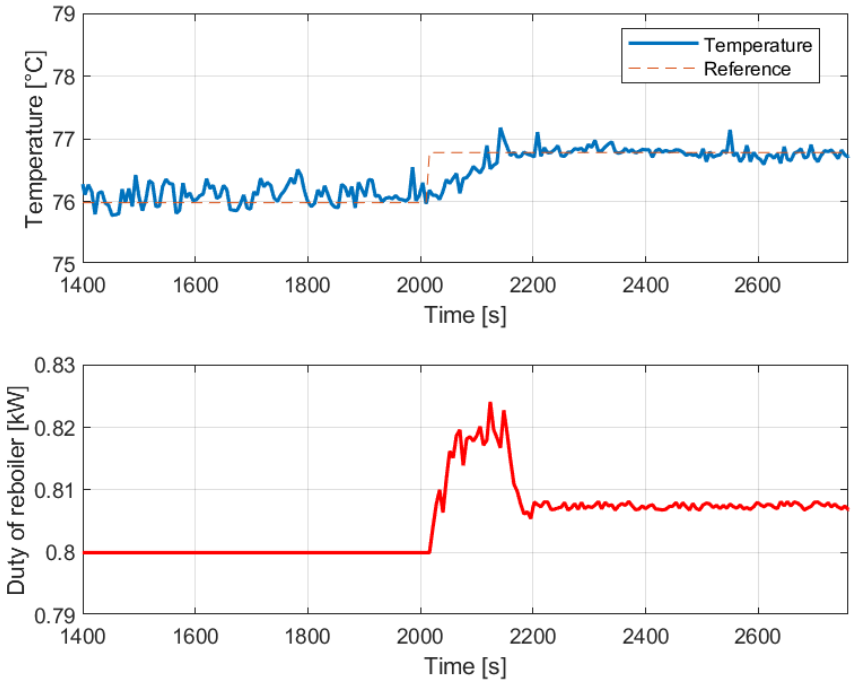

Figure 3.21: Reference tracking of temperature on the bottom of column (top) with input signal (bot).

In Figure 3.21 the dependence of the temperature at the bottom of the column and the control action duty of the reboiler applied to a real laboratory column is shown. The temperature stabilized after 200 seconds from the step change and oscillated around the setpoint with a small amplitude. Before the LQR controller was activated, temperature fluctuations were observed due to external factors such as pressure or ambient temperature changes, but after applying the control, these oscillations are much lower, which highlights the regulator's effectiveness. Compared to LQR simulation we got smaller overshoot and compared to the PI controller, the control action of duty of reboiler has a smaller overshoot too by 0.4 kW of energy, so the implementation of LQR can save us the financial resources needed to run the column. In addition, the temperature T_8 reaches the setpoint in a faster time by 75% than with the PI controller, demonstrating the interaction between the input variables and the efficiency of LQR in MIMO systems.

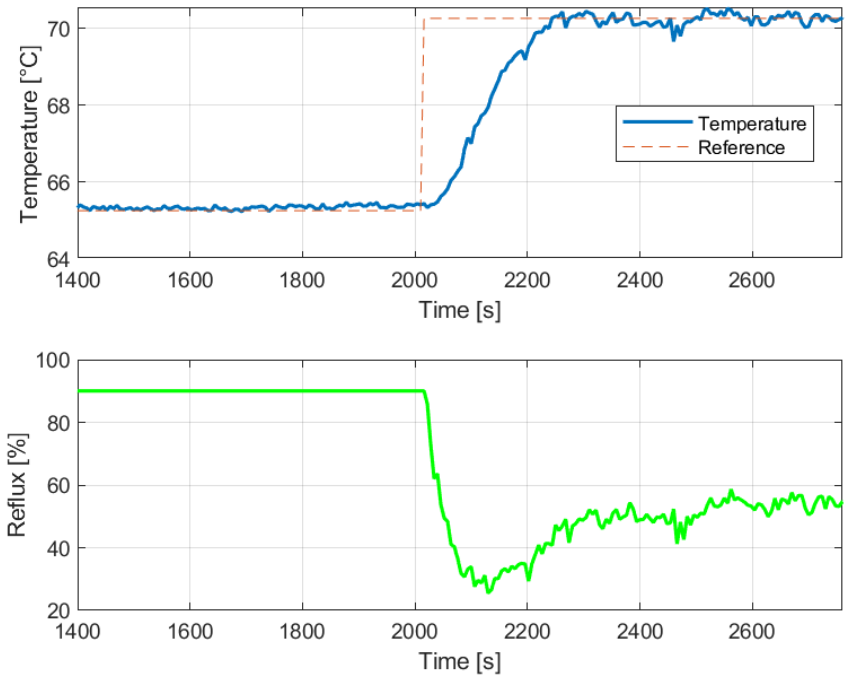

Figure 3.22: Reference tracking of temperature on the top of column (top) with input signal (bot).

In Figure 3.22 we can see the dependence of the temperature at the top of the column and the control action of the reflux applied to a real laboratory column. Similar to the temperature at the bottom of the column, the temperature at the top becomes stable after approximately 200 seconds from step change. Compared to LQR simulation undershoot in reflux is higher but compared to PI control the control action of the reflux is not so aggressive and does not fall down immediately but decreases more smoothly which may help avoid valve damage.

Chapter 4

Conclusions

This work has presented a study of the UOP3CC Continuous Distillation Column, focusing on its operation, modeling, and control.

The modeling was performed using AVEVA process simulation and gPROMS process builder. An important benefit of using these softwares is the ability to estimate internal process parameters or variables that cannot be directly measured on the laboratory column, such as compositions or vapor/liquid flow rates, reflux flow rates, or duty of condenser. These simulations not only validated the experimental data but also highlighted the potential of process modeling as a tool for system analysis and optimization.

The practical implementation of PI controllers for the regulation of temperature in the top and bottom trays of the column demonstrated the effectiveness of the Skogestad tuning method in achieving the desired setpoints. The experimental data validated the performance of the control system, ensuring stable and efficient operation of the distillation process.

To improve performance a Linear Quadratic Regulator (LQR) was designed since the distillation column is a multivariable system with multiple manipulated and controlled variables, the use of LQR was properly due to its ability to handle MIMO systems in a coordinated way. For unmeasurable states, it was necessary to design a state observer which allowed for the estimation of states not directly measurable. Compared to PI, the LQR controller demonstrated smoother control actions and better coordination between manipulated variables, resulting in improved temperature tracking with reduced aggressiveness in reflux control, faster settle time, and energy savings. The overshoot in the duty of reboiler was reduced by 0.4 kW and the settling time at T_8 temperature by 75%.

The successful integration of experimental and simulated data highlight the importance

of combining physical experimentation with modeling and simulation for process analysis. The results of this thesis provide a foundation for future advances in the control and modeling of distillation systems.

Future Work

Although the control using a discrete PI regulator and a discrete LQR regulator provides promising results, there is still a lot of room for experimentation. It is possible to experiment with the weights in the LQR controller to achieve a smaller overshoot in the duty of the reboiler and a smoother control action of the reflux. One possible extension is the implementation of model predictive control, which could offer improved performance by explicitly handling constraints and predicting future system behavior over a defined horizon. Its use could lead to improved tracking performance, constraint satisfaction, and energy savings.

Appendix A

Resumé

Diplomová práca sa venuje návrhu, implementácii a porovnaniu riadiacich stratégií pre laboratórnu destilačnú kolónu UOP3CC, pričom hlavným cieľom je zabezpečiť stabilnú a efektívnu reguláciu teplôt v hornej (T_1) a dolnej (T_8) časti kolóny prostredníctvom manipulácie s dvoma vstupmi: výkonom varáka a refluxným pomerom. Vzhľadom na viacvstupovo-výstupový (MIMO) charakter systému, nelinearity a silné prepojenie medzi premennými, si návrh regulátora vyžaduje dôslednú analýzu systému a vhodné modelovanie.

Destilácia patrí medzi najrozšírenejšie separačné metódy v chemickom a potravinárskom priemysle. Je založená na rozdielnej prchavosti zložiek v kvapalnej zmesi, kde dochádza k separácii komponentov na základe rozdielnych bodov varu. V rektifikačnej kolóne prebieha táto separácia v protiprúdnom usporiadaní pár-kvapalina, pričom kvapalina tečie nadol a para stúpa nahor. V ustálenom stave sa medzi jednotlivými stupňami kolóny vytvárajú rovnovážne podmienky, ktoré vedú k obohacovaniu jednej zložky v destiláte a druhej v zvyšku.

Presnosť a stabilita teplotného profilu je kľúčová pre kvalitu separácie, preto je návrh riadiaceho systému nevyhnutný pre optimálne fungovanie kolóny. V priemyselných podmienkach tvorí spotreba energie na destiláciu značnú časť celkových nákladov, čo ďalej zvyšuje význam účinnej regulácie.

Pre návrh riadiaceho systému je nevyhnutné pochopiť dynamické správanie procesu. V práci bola preto vykonaná experimentálna identifikácia dynamiky reálnej kolóny. Po krokových zmenách na vstupoch (zmena výkonu varáka a refluxu) boli zaznamenané výstupné teploty a následne spracované v prostredí MATLAB. Pomocou metódy subspace identifikácie (N4SID) bol odvodený lineárny stavovo-priestorový model so štyrmi stavmi, dvoma vstupmi a dvoma výstupmi. Tento model sa neskôr využil ako základ pre návrh PI a LQR regulátora. Presnosť modelu bola overená výpočtom metriky RMSE (Root Mean Square Error), ktorá potvrdila, že odvodený model je

dostatočne presný na návrh regulátora. Model bol tiež implementovaný do Simulinku, čím sa vytvoril základ pre testovanie riadiacich algoritmov.

Ako prvý bol navrhnutý klasický PI (proporcionálno-integračný) regulátor, ktorý patrí medzi najrozšírenejšie typy riadenia v priemysle. PI regulátor koriguje chybu medzi žiadanou a skutočnou hodnotou výstupu kombináciou proporcionálnej a integračnej akcie. Na rozdiel od PID regulátora neobsahuje deriváciu, čím sa znižuje náchylnosť na šum v signále.

Ladenie PI regulátorov bolo vykonané pomocou Skogestadovej metódy, ktorá umožňuje rýchly výpočet PI parametrov na základe prenosovej funkcie systému. V práci boli získané prenosové funkcie medzi výstupmi (T_1), (T_8) a vstupmi, ktoré slúžili ako podklad pre výpočet Kp a Ti. Výsledky simulácií ukázali, že PI regulácia je schopná stabilizovať systém, avšak vykazuje nadmerné zásahy najmä v oblasti refluxu a prekmyt vo výkone varáka. Rýchle zmeny riadiacich signálov by mohli v reálnych podmienkach poškodzovať technické komponenty (napr. regulačné ventily) alebo čo sa týka výkonu varáka zvyšovať energetické náklady .

Z dôvodu prepojenosti veličín a charakteru systému ako MIMO bola navrhnutá pokročilejšia riadiaca stratégia typu LQR (Linear Quadratic Regulator). LQR predstavuje optimalizačný prístup ku spätnej väzbe, pri ktorom sa minimalizuje kvadratická nákladová funkcia. V práci bolo toto riadenie rozšírené o integrálny člen pre zabezpečenie nulovej trvalej regulačnej odchýlky. Po rozšírení stavového opisu bol návrh regulátora realizovaný v prostredí MATLAB pomocou funkcie dlqr.

LQR umožňuje koordinované riadenie oboch vstupov súčasne – napríklad v prípade, že reboiler má príliš silný vplyv, môže LQR automaticky preferovať menej agresívny zásah cez reflux. Práve táto koordinácia je výhodou oproti nezávislým PI slučkám.

Vzhľadom na to, že nie všetky stavy modelu sú merateľné, bol súčasťou návrhu aj diskrétny stavový pozorovateľ. Ten umožňuje odhad nepozorovateľných veličín na základe známeho modelu a meraných výstupov. V práci bol navrhnutý pomocou funkcie dlqe a jeho výkonnosť bola overená porovnaním skutočných a odhadovaných stavov. Pozorovateľ zabezpečuje robustnosť voči šumu a modelovým nepresnostiam a je nevyhnutnou súčasťou stavovej spätnej väzby.

Simulačné výsledky ukazujú, že LQR regulácia poskytuje plynulejšie a efektívnejšie riadenie ako PI regulátory. Zatiaľ čo PI regulátor spôsoboval oscilácie a skokové zmeny v riadiacich signáloch, LQR umožňoval hladké prechody s minimálnym prekmitom. Významným prínosom bolo zníženie agresivity v oblasti refluxu a efektívnejšia

spolupráca oboch vstupov, čo spôsobilo aj menší prekmit vo výkone varáka. Správnou voľbou váhovacích matíc bolo možné reguláciu prispôsobiť požiadavkám na technické obmedzenia systému.

Táto práca dokazuje, že aj v laboratórnych podmienkach je možné efektívne aplikovať pokročilé riadiace algoritmy, akými sú stavové regulátory. Okrem klasického PI prístupu bol úspešne implementovaný a otestovaný LQR regulátor so stavovým pozorovateľom. Simulácie ukázali, že pri správne navrhnutom modeli možno dosiahnuť výrazné zlepšenie regulácie, zníženie energetických nákladov a zvýšenie stability systému. Práca predstavuje spojenie teoretických poznatkov z oblasti riadenia, modelovania a optimalizácie s praktickou aplikáciou v reálnom procese a poskytuje cenné základy pre ďalší vývoj riadiacich systémov pre separačné procesy.

Bibliography

[1] Alan Brown. *Distillation Concepts and Applications.* Industrial Press, 2018.

[2] Michael Carter. *Efficiency in Distillation Operations.* Tech Books, 2017.

[3] Frederico da Conceição do Carmo Montes. Simulation and optimisation of batch distillation operations. Master's thesis, Instituto Superior Técnico Lisboa, Lisbon, Portugal, 12. 2015.

[4] A. Gorak and E. Sorensen. *Distillation: Fundamentals and Principles.* Handbooks in Separation Science. Academic Press, 2014.

[5] Mohamed Hamdy, Abdalhady Ramadan, and Belal Abozalam. Comparative study of different decoupling schemes for tito binary distillation column via pi controller. *IEEE/CAA Journal of Automatica Sinica*, 5(4):869–877, 2018.

[6] Charles R. Johnson and Helene M. Shapiro. Mathematical aspects of the relative gain array. *SIAM Journal on Algebraic Discrete Methods*, 1986.

[7] A.A. Kiss. *Advanced Distillation Technologies: Design, Control and Applications.* Wiley, 2013.

[8] Henry Z. Kister. *Distillation design.* California, 1992.

[9] Carl Knospe. Pid control. *Control Systems Magazine, IEEE*, 26:30– 31, 03 2006.

[10] Zhigang Lei, Chengyue Li, and Biaohua Chen. Extractive distillation: a review. *Separation & Purification Reviews*, 32(2):121–213, 2003.

[11] Yun Li, Kiam Heong Ang, and G.C.Y. Chong. Pid control system analysis and design. *IEEE Control Systems Magazine*, 26(1):32–41, 2006.

[12] Armfield Limited. *UOP3CC Dsitilation Column Documentation.* Weest Street, Hampshire, 2010.

[13] Siemens Industry Software Limited. *gPROMS Process Documentation*. 26-28 Hammersmith Grove, London W6 7HA, 2023.

[14] Y. Liu and S. Wang. Application of nrtl model for phase equilibrium in distillation. *Industrial Engineering Chemistry Research*, pages 2020–2028, 2005.

[15] W.L. Luyben. *Practical Distillation Control*. Springer US, 2012.

[16] T. Mészárosová. Advanced control of a laboratory distillation column. Diplomová práca, ÚIAM FCHPT STU v Bratislave, Radlinského 9, 812 37 Bratislava, 2023.

[17] Nicoleta Nicolae, Marian Popescu, and Cristian Patrascioiu. Implementation of advanced process control in refineries. In *2019 23rd International Conference on System Theory, Control and Computing (ICSTCC)*, pages 95–100, 2019.

[18] DrSc Prof. Ing. Miroslav Fikar. State-space discrete-time control design. Prezentácia na predmete Teória automatického riadenia 2, 2024.

[19] J. D. Seader and E. J. Henley. *Separation Process Principles: Chemical and Biochemical Operations*. Wiley, Hoboken, NJ, 3rd edition, 2017.

[20] Gembong Edhi Setyawan, Wijaya Kurniawan, and Amroy Casro Lumban Gaol. Linear quadratic regulator controller (lqr) for ar. drone's safe landing. In *2019 International Conference on Sustainable Information Engineering and Technology (SIET)*, pages 228–233, 2019.

[21] Sigurd Skogestad. *Multivariable Feedback Control: Analysis and Design*. Wiley, New York, 2nd edition, 2005.

[22] John Smith and Jane Doe. Principles of raoult's law in distillation. *Chemical Engineering Journal*, 5:123–130, 2020.

[23] Mark Taylor. Understanding reflux ratios in distillation. *Journal of Separation Science*, pages 78–85, 2021.

[24] Ústav informatizácie, automatizácie a matematiky. Uop3cc: Rektifikačná kolóna armfield, 2023.